IOP Conf. Series: Materials Science and Engineering **350** (2018) 012004 doi:10.1088/1757-899X/350/1/012004

Effect of Long Selenization Time on Co Films under a Low Temperature of 300 ℃ to Synthesize a Nanostructure $CoSe_2$ and Optical Properties

PO-FENG WU[1,a], JEN-BIN SHI[2,b*], BO-CI CHENG[2,c], CHENG-HAN WU[2,d], HSUAN-WEI LEE[2,e], HSIEN-SHENG LIN[2,f], FU-CHOU CHENG[3,g], KUAN-PING CHEN[2,h]

1College of general education, Hung-Kuang University, No. 1018 Sec. 6, Taiwan Boulevard, Shalu District, Taichung City 4330, Taiwan

2Engineering, Feng Chia University, No.100, Wenhwa Rd., Seatwen, Taichung 40724, Taiwan

3Professor & Director in Stem Cell Center, Department of Medical Research, Taichung Veterans General Hospital, No. 160, 3rd Section, Taichung Harbor Road, Taichung 40705, Taiwan

Email:[a]gavinwu0325@gmail.com,[b*]jbshi@fcu.edu.tw,[c]bochi0020@gmail.com,[d]sasabi96541@gmail.com,[e]rocklee3001g@gmail.com, [f]shemglin@ms63.hinet.net, [g]fucheng@vght.gov.tw, [h]debby200598@gmail.com

Abstract. This work investigates a simple and non-toxic method to transform pre-deposited amorphous Co film into $CoSe_2$ films at a fixed, low temperature of 300 ℃. Single $CoSe_2$-phase films having good crystallinity were obtained at a selenisation time ≧ 24 hours. A nanostructure $CoSe_2$ having two different nano-morphological layers was observed. The $CoSe_2$ films (72 hours) observed a large absorption and a direct band gap.

1. Introduction

Transition metal chalcogenides/dichalcogenides MX_2 (M = Mn, Fe, Ni, Co; X = S, Se, Te) has been investigated on their optical, magnetic, and electrical properties [1–4]. Many theoretical and experimental reports have been done on the pyrites MX_2 [5–7]. Due to the application in, rechargeable battery electrodes [8] and their potential applications in such areas as spintronic devices pyrites MX2[9]. CoSe2 and CoSe have received increasing appeal as potential cathodic catalysts for fuel cells [10-13]. Fuel cells can directly reduce our dependence on oil, energy use, and harmful emissions, which are used for stationary, portable power, and transportation. In the other hand, the oxygen reduction reaction (ORR), used in an acid medium Pt-based material, is the best and most used catalyst.

Content from this work may be used under the terms of the Creative Commons Attribution 3.0 licence. Any further distribution of this work must maintain attribution to the author(s) and the title of the work, journal citation and DOI.
Published under licence by IOP Publishing Ltd

However, Pt materials are too expensive, while Fe and Co metals are much cheaper and serve equally as potential catalytic centers towards ORR in the creation of solar cell material. The cathodic oxygen reduction in chalcogenides of various transition metals has been further reported [14-16].

As an important pyrite-type compound, $CoSe_2$ has been known as a potential cathodic catalyst [14-16]. However, the extraordinary optical capability of $CoSe_2$ has not much been investigated for its potential application as a solar cell material of $CuInSe_2$ [17,18].

In this study, we demonstrated a simple and non-toxic method for direct low temperature synthesis of the $CoSe_2$ films with nanostructures. Transition metal dichalcogenides have been composited by using the direct stoichiometric combination of component in evacuated quartz ampoule [7]. However, as a result of the limit of slow diffusion, the whole response needs to operate at a high temperature from 500 to 1200 ℃, and intermittent grinding [7]. No report is available for $CoSe_2$ thin film growth by selenization of cobalt films. This process runs at a low temperature of 300 ℃, but requires a great deal of time. In this study, our aim is to further investigate the synthesis, structure, composition, and morphology of $CoSe_2$ films. The evolution of the optical properties of $CoSe_2$ is also discussed.

2. Detail Experimental

The $CoSe_2$ thin films were deposited onto the glass by selenization. In our work, the DC magnetron sputtering system was used to fabricate Co precursors. Co thin films were grown on the glass substrates and the chamber was initially evacuated to a base pressure of about 2.0×10^{-5} Torr. The Ar working pressure was 2.0×10^{-3} Torr and the DC power was 70 W for 1 hour. The Co target (99.95 % purity) was then presputtered for 10 minutes to remove any contaminants, especially oxide layering, on the surface of the Co target. 600 nm Co films were formed on the substrate at a deposition rate of 10 nm/minute.

All samples were put into a glass tube with pure Se powder when the Co precursors were fabricated. The glass tube was evacuated by using a pump, then placed in a furnace. The samples were then selenized in the furnace at 300 ℃ for 2, 5, 10, 24, and 72 hours. The phase and crystallization structure were treated by X-ray diffraction (XRD, SHIMADZU XRD-6000) utilizing Cu K_α radiation. In the course of observing the structure and morphology, the samples were used by a field-emission scanning electron microscope/energy dispersive spectrometer (FE-SEM/EDS, HITACHI S-4800). The optical absorption analysis of the $CoSe_2$ thin film was measured on a UV/Visible/NIR spectrophotometer (HITACHI U-3501).

3. Results and Discussion

Figure 1 shows the XRD patterns of the Co films selenized as a function of selenization time. The Co films and pure Se were annealed in a vacuum ($< 2 \times 10^{-5}$ Torr) sealed tube at different selenization times (2, 5, 10, 24, and 72 hours). Usually, there are three stable phases and they are homogeneous at room temperature ($Co_{0.85}Se$, CoSe and $CoSe_2$) and two other possible compositions (Co_2Se_3 and Co_3Se_4) for cobalt selenides [19-22].

The XRD pattern (Figure 1) of Co films as the starting precursor (0 hour) displayed an amorphous structure that does not show any peaks in the XRD diffraction pattern. These XRD patterns are very monotonic, and below 10 hours of selenization, they also show the presence of only two phases, whose peaks are marked with closed stars (CoSe phase) and squares ($CoSe_2$ phase). Phase one was indexed to the CoSe phase, identified as JCPDS card number 15-464, which has a hexagonal structure.

The other diffraction peaks can be indexed to the phase of the $CoSe_2$ hexagonal structure, which matches with the standard data file of $CoSe_2$. The XRD patterns (selenization time of 10 hours) showed no Se peaks, and the CoSe and $CoSe_2$ (Co/Se ratio ~ 1.7) phases coexisted. As the selenization time increased, the thickness and crystallinity of the films also increased; their peaks were sharper, and their intensities were drastically enhanced. The XRD patterns (Figure 1) were completely transformed into $CoSe_2$ after further thermal treatment (selenization time ≥ 24 hours). XRD patterns also showed the appearance of single phase $CoSe_2$. The $CoSe_2$ peak intensities corresponded to those in PDF 89-2002, and showed a good crystallinity. No peaks from other phases could be detected.

Surface and cross-sectional morphological images of the precursor Co films and the Co-Se films prepared from different selenization times are shown in Figure 2. The composition of the films has been estimated from energy dispersive analysis of X-rays (EDAX). At selected areas, the Se/Co atomic molar ratios obtained from cross sectional EDAX analysis in the upper/lower layers and the thicknesses of films are shown in Figure 3, as a consequence of the different selenization times. The EDAX results, at the upper layers, revealed the following composition in atomic ratio, where Se/Co ratios are above 1: atomic ratio of Se/Co of ~ 1.3 for film selenized at 5 hours; and ~ 1.7 for film selenized at 10 hours. The films selenized at 5 or 10 hours have a deficiency of Se content (selenization time ≤ 10 hours). The reaction that leads to the formation of the mixture of CoSe and $CoSe_2$ is favored in the upper layers. There are many nano-dots in the surface layer at a selenization time of 2 hours (Figure 2c & 2d). A layered structure was observed (Figure 2e – 2h) for the selenization times of 5 and 10 hours. The upper layer is composed of a mixture of CoSe and $CoSe_2$ phases. The lower layer corresponds to the Co phase due to EDAX results (Se/Co ~ 0). This presumption may be acceptable because the selenization process starts at the surface. The film in the upper layers thickens with an increase in selenization time (Figure 3), due to more selenium atoms with high activity diffusing into the crystal lattice of the Co-Se system. The amorphous structure in the precursor films can completely evolve into granular $CoSe_2$ grains through long selenization time (≥ 24 hours). The nano-sized scale of $CoSe_2$ grains can be observed clearly in the films. The average size of the grains is within a range of 10 to 60 nm. The SEM surface and cross-sectional views of selenized films at a selenization time of ≥ 24 hours (Figure 2j and 2l) also showed a layered nano-structure. The upper layer is composed of the $CoSe_2$ phase, which has a large uniform area and nano-porous crystallite structure ($CoSe_2$-p). The lower layer is composed of a dense, nano-sized cylindrical crystallite structure ($CoSe_2$-d), and closely corresponds to stoichiometric $CoSe_2$ phases. Conversely, the upper layer absolutely corresponds to non-stoichiometric $CoSe_2$ phases, but the Se was found to be richer with an Se/Co ratio of ~ 2.2. As shown in Figure 2i -2l, two layers can be clearly found on the nano-structure $CoSe_2$ film. Those results are consistent with the X-ray diffraction analysis of the sample with a phase corresponding to $CoSe_2$.

The optical characteristic of the $CoSe_2$ film for 72 hours was measurement by optical absorption utilizing UV spectrophotometer. The absorption coefficient (α) is connected to photon energy ($h\nu$) by the following equation [23]:

$$(\alpha h\nu)^{m} = A(h\nu - E_g) \quad (1)$$

where h is the Plank constant, A is a constant, E_g is the band gap, and m takes the value 1/2 and 1/3 for indirect allowed and indirect forbidden, value 2 for direct allowed transition, and value 2/3 for direct

forbidden, respectively. The transition in the thin film can be determined by plotting $(\alpha h\nu)^m$ against photon energy $h\nu$ for a suitable value of "m", which leads to having a direct line. The value of E_g is obtained by extrapolating the linear portion of the graph to intercept the photon energy axis.

The type of transition is neither indirect nor direct, owing to the fact that there are no straight lines in any of the plots for $(\alpha h\nu)^{2/3}$ versus hv, $(\alpha h\nu)^{1/3}$ versus $h\nu$, and $(\alpha h\nu)^{1/2}$ versus $h\nu$. After 72 hours of selenization, the $CoSe_2$ thin film is a direct allowed transition. Through extrapolation of the linear portion of the plots drawn for $(\alpha h\nu)^2$ versus $h\nu$ to the energy axis, the band gap of the film was ascertained. The optical band gap is 1.51 eV, as depicted in Figure 4. A similar result for previous researchers in optical absorption measurement have reported by Maneeprakorn et al. [24], who have found that the direct band gap of orthorhombic $CoSe_2$ nanoparticles was 1.45 eV. Figure 4 (insert) displays the absorption coefficient values of the $CoSe_2$ film (for 72 hour samples), which are between 1.0×10^5 to 2.0×10^5 cm^{-1}

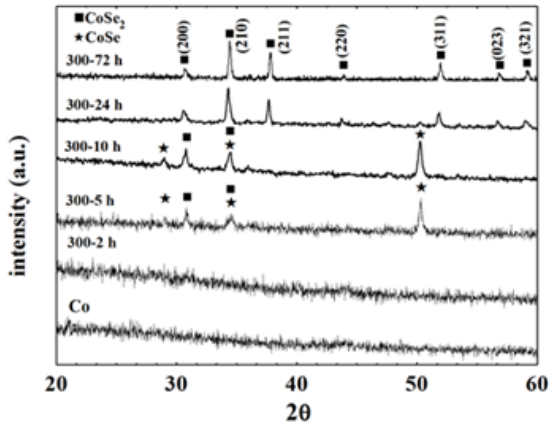


Figure. 1. The XRD patterns of samples selenized at 300 ℃ for different time.

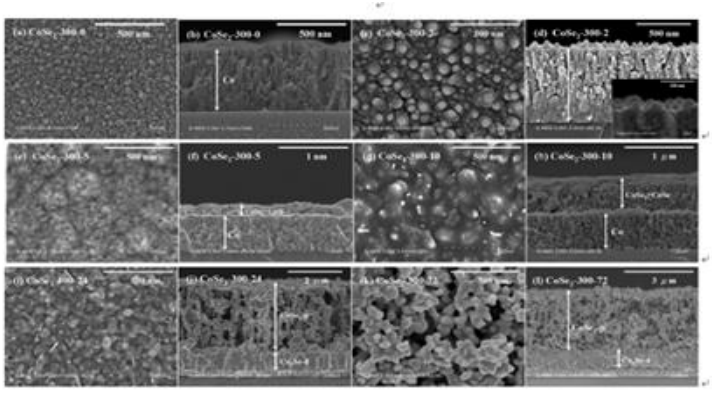


Figure. 2. FE-SEM images of top view and cross-sectional view of (a), (b) Cobalt thin films ($CoSe_2$-300-0); (c), (d) selenized at 300 ℃ for 2 hours ($CoSe_2$-300-2); (e), (f) selenized at 300 ℃ for 5 hours ($CoSe_2$-300-5); (g), (h) selenized at 300 ℃ for 10 hours ($CoSe_2$-300-10); (i), (j) selenized at 300 ℃ for 24 hours ($CoSe_2$-300-24); (k), (l) selenized at 300 ℃ for 72 hours ($CoSe_2$-300-72).

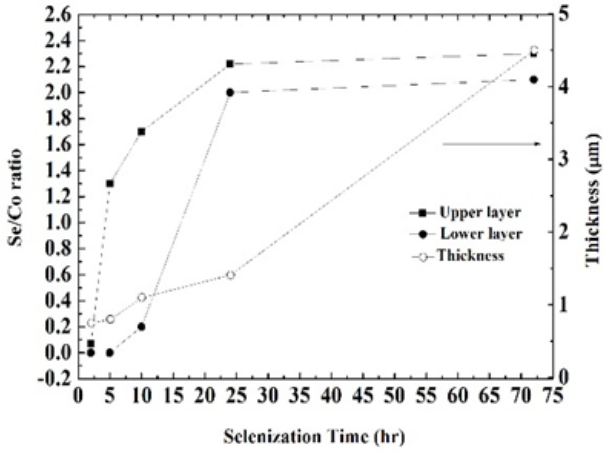


Figure. 3. The Se/Co atomic ratio of samples on the cross-section prepared at 300 ℃ for different length of time.

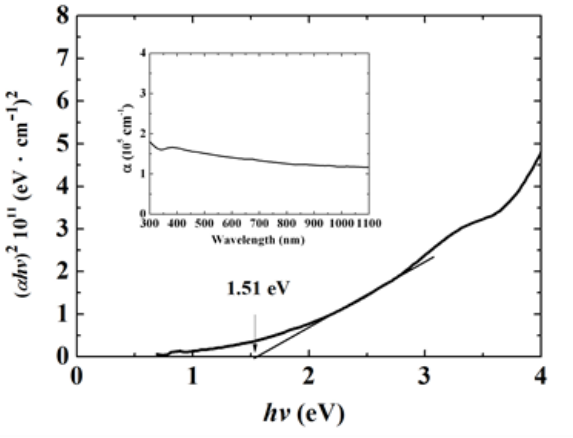


Figure. 4. The plots of (α hv)2 versus hv with absorption coefficient(inset) for CoSe2 thin films prepared at 300 ° C for 72 hours.

4. Conclusions

In summary, we demonstrate that this long lasting (up to ~ 3 days) method of selenization on Co films, using non-toxic pure Se at a low and fixed temperature of 300 ℃, to obtain the nanostructed $CoSe_2$. When selenization occurs within a shorter time (≤ 10 hours), due to the limit of Se's very slow diffusion speed under low temperature, the $CoSe_2$ phase does not form completely. However, the Co film still exists on the bottom layers. Within this time frame, the selenization time rises and the Co-Se mixture films becomes thicker, and the CoSe and $CoSe_2$ phases become more dominant. With a selenization time ≥ 24 hours, a single $CoSe_2$ phase having good crystallinity was obtained throughout the films' thickening. SEM surface and cross sectional views show that $CoSe_2$ films have a nanostructure of two different morphological layers. Absorption measurements show that $CoSe_2$ films have a large absorption coefficient ($\alpha > 1.0 \times 10^5$ cm^{-1}) and a direct gap of about 1.51 eV. The nanostructure $CoSe_2$ film shows a direct band gap and high absorption coefficient.

5. References

[1] H.S. Jarrett, W.H. Cloud, R.J. Bouchard, S.R. Butler, C.G. Frederick and J.L. Gilson: Phys. Rev. Lett. Vol. 21（1968）, p. 617.
[2] P. Panissod, G. Krill, M. Lahrichi and M.F. Lapierre: Phys. Lett. A Vol. 59（1976）, p.221.
[3] S.M. Marcus and T.A. Bither: Phys. Lett. A Vol. 32（1970）p. 363.
[4] K. Adachi, K. Sato and M. Takeda: J. Phys. Soc. Jpn. Vol. 26（1969）, p. 631.
[5] G. Krill and A. Amamou: J. Phys. Chem. Sol. Vol. 41（1980）, p. 531.
[6] V.H. McCann and J.B. Ward: J. Phys. Chem. Sol. Vol. 38（1977）, p. 991.
[7] H. Sato, F. Nagasaki, Y. Kani, S. Senba, Y. Ueda, A. Kimura and M. Taniguchi: Solid State Commun., Vol. 118 (2001), p. 563.
[8] L. Levy, N. Feltin, D. Ingert and M.P. Pileni: J. Phys. Chem. B Vol. 101 (1977), p. 9153.
[9] S.A. Wolf, D.D. Awschalom, R.A. Buhrman, J.M. Daughton, S.V. Molnar, M.L. Roukes, A.Y. Chtchelkanova and D.M. Treger: Science Vol. 294 (2001), p. 1488.
[10] R.A. Sidik and A.B. Anderson: J. Phys. Chem. B Vol. 110 (2006), p. 936.

[11] E. Vayner, R.A. Sidik, A.B. Anderson and B.N. Popov: J. Phys. Chem. C Vol. 111 (2007), p. 10508.
[12] D. Susac, A. Sode, L. Zhu, P.C. Wong, M. Teo, D. Bizzotto, K.A.R. Mitchell, R.R. Parsons and S.A. Campbell: J. Phys. Chem. B Vol. 110 (2006), p. 10762.
[13] M.R. Gao, Q. Gao, J. Jiang, C.H. Cui, W.T. Yao and S.H. Yu: Angew. Chem. Int. Ed. Vol. 50 (2011), p. 4905.
[14] L. Zhu, D. Susac, M. Teo, K.C. Wong, P.C. Wong, R.R. Parsons, D. Bizzotto, K.A.R. Mitchell and S.A. Campbell: J. Catal. 258, p. 235-242.
[15] Y.J. Feng, T. He and N.A.Vante: Chem. Mater. Vol. 20 (2008), p. 26.
[16] Y. J. Feng, T. He and N.A. Vante: Fuel Cells Vol. 10 No.1 (2010), p.77.
[17] J.B. Shi, Y.C. Chen, P.F. Wu, S.Y. Yang, T.K. Kang, P.C. Yang, C.L. Lin, S.L. Young and M.C. Kao: Res. Technol. Vol. 48 (2013), p. 94.
[18] J.B. Shi, Y.C. Chen, C.J. Chen and P.F. Wu: Cryst. Res. Technol. Vol. 47 (2012), p. 183.
[19] M. Hansen: Constitution of Binary Alloys, Geminuim Publishing Company, New York (1985), p. 502-503.
[20] X.H. Liu, N. Zhang, R. Yi, G.Z. Qiu, A.G. Yan, H.Y. Wu, D.P. Meng and M.T. Tang: Mater. Sci. Eng. B, Vol. 140 (2007), p. 38.
[21] J.H. Zhan, X.G. Yang, S.D. Li, Y. Xie, W.C. Yu and Y.T. Qian: J. Solid State Chem. Vol. 152 (2000), p. 537.
[22] J.F. Zhao, J.M. Song, C.C. Liu, B.H. Liu, H.L. Niu, C.J. Mao, S.Y. Zhang, Y.H. Shen and Z.P. Zhang: Cryst. Eng. Commun. Vol. 13 (2011), p. 5681.
[23] J. C. Osuma, C. I. Oriaku, F. I. Ezema and F. I. Ezema: Chalcogenide Lett. Vol. 6 (2009), p. 385.
[24] W. Maneeprakorn, M. A. Malik and P. O'Brien: J. Mater. Chem. Vol. 20 (2010), p. 2329.

Acknowledgments

This research was supported by the National Science Council of R.O.C. under grant No. MOST 105-2623-E-035-002-ET, MOST 105-2221-E-035-073, TCVGH-FCU1068202, MOST 106-2221-E-035-082 and the Precision Instrument Support Center at Feng Chia University.